JNEST EISSN: 2961-8738 ● PISSN: 2961-8916 ● DOI: 10.56741/jnest.v5i01.1376 35
Article Received 10 September 2025, Revised 16 November 2025

Multi-Response Optimization of 1 Kg Mass Artifact and Gravimetry as A Control Process in Legal Metrology Mass Laboratories Using the Taguchi Method and Response Surface Methodology

Saufik Luthfianto*, Sandi Satria, and Irfan Santosa

***Abstract*— Artifacts are instruments used as reference standards or objects agreed upon at the national level. The reference standard must have a degree of accuracy based on measurements conducted by competent personnel. Another standard involves laboratory support facilities, including proper temperature, humidity, and lighting conditions. The purpose of applying standards is to minimize measurement errors and uncertainties. Therefore, standards in Legal Metrology ensure that all measuring instruments are traceable in terms of accuracy, both nationally and internationally. However, if the intercomparison results of a region fall outside the upper and lower limits in terms of artifact output, it is considered a failure, requiring room temperature standardization based on the optimal value of artifact actualization. The research method used is the Taguchi method combined with response surface methodology. This method is one of the mathematical approaches to quality control and is applied from the earliest stage, namely the design phase. The orthogonal array used is $L_8(2^4)$. The response measured is the actualization of a 1-kilogram special accuracy class weight artifact and gravimetry. The controlled and varied independent variables include AC temperature, actualization duration, lighting intensity, and the number of operators in the laboratory. Currently, the optimization process of laboratory conditions is still performed manually by laboratory operators, making it difficult to control the independent variables. Therefore, this study will implement the Internet of Things (IoT) to assist operators in setting independent variables for laboratory conditions. The research results show that the optimal conditions include an AC temperature of 16°C, an actualization duration of 15 minutes, 50% lighting intensity, and 1 operator in the laboratory.**

***Index Terms*— Artifact, Gravimetry, Multi-Response Optimization, Reference Standard.**

INTRODUCTION

One of the most prevalent challenges faced by laboratories is the control of independent variables that can significantly influence the quality and stability of objects within them. These variables include temperature fluctuations, humidity levels, air pressure variations, and electromagnetic interference, all of which can cause deviations in measurement accuracy. The absence of standardized laboratory environmental conditions leads to inconsistent test results and increased variability in measurement data. Over time, these uncontrolled environmental factors contribute to quality degradation in artifacts, calibration standards, and other reference materials used in laboratory assessments. In metrology, quality is inversely related to variability, meaning that the lower the variability in measurement processes, the higher the quality and reliability of results [1]. When laboratories fail to maintain stable conditions, variations in test results become more pronounced, leading to inaccurate calibrations, unreliable measurements, and increased uncertainty in traceability chains. This issue is particularly concerning in legal metrology laboratories, where precise and repeatable measurements are critical for ensuring fair trade practices, industrial compliance, and regulatory enforcement.

A notable consequence of these uncontrolled variables is the declining quality of test results for metrological artifacts, which has been observed in several laboratories. This decline directly impacts laboratory intercomparison scores, reducing the level of agreement between different institutions and affecting the overall credibility of measurement results. Poor intercomparison performance indicates systematic inconsistencies across laboratories, making it difficult to establish universally accepted measurement standards. To address these challenges, concrete efforts must be implemented through research focusing on the automation of laboratory environmental controls. The integration of advanced sensor networks, real-time monitoring systems, and AI-driven automation can significantly enhance the stability of laboratory conditions, thereby minimizing variability, improving measurement accuracy, and strengthening the reliability of test results across different metrology institutions.

Data from the Ministry of Trade indicate that the intercomparison scores of artifacts in metrology laboratories across the Java, Madura, Bali, and East Nusa Tenggara (NTT) regions in 2022 showed an average En Ratio score below the reference value. The En Ratio (Error Normalized Ratio) is a key metric in metrological comparisons, used to evaluate the level of agreement between laboratory measurements and established reference values. A lower-than-expected En Ratio suggests potential discrepancies in measurement consistency and accuracy, which can lead to uncertainties in the calibration of standard artifacts [2].

The quality of metrological artifacts plays a fundamental role in ensuring the accuracy and traceability of various measuring, weighing, and metering instruments (UTTP) used in trade and industrial sectors. These

Saufik Luthfianto (Corresponding author) is with the Industrial Engineering Study Program, Universitas Pancasakti Tegal, Tegal, Central Java, Indonesia. **Sandi Satria** is with the Technical Implementation Unit, Legal Metrology Office, Tegal City, Indonesia. **Irfan Santoso** is with the Mechanical Engineering Study Program, Universitas Pancasakti Tegal, Tegal, Central Java, Indonesia. Correspondence: saufik_lutfianto@upstegal.ac.id,

© 2026 IISTR

instruments function as transaction tools in commercial activities, where even minor inconsistencies in calibration can have significant financial and operational consequences. The traceability chain, which ensures that all measurement instruments adhere to internationally recognized standards, is heavily dependent on the reliability of artifacts maintained in metrology laboratories. When artifact quality varies significantly, the accuracy of derived measurement quantities, such as mass, volume, and length, can be compromised. This variability can lead to measurement errors in commercial transactions, affecting fair trade, taxation, and regulatory compliance. Moreover, industries that rely on high-precision measurements, such as pharmaceuticals, aerospace, and manufacturing, may experience production inefficiencies, increased wastage, and potential safety risks due to inconsistencies in measurement standards.

To address these issues, maintaining artifact integrity through regular calibration, environmental control, and adherence to international metrology standards is essential. Implementing standardized quality assurance procedures, improving laboratory competence, and enhancing collaboration among regional metrology institutions can significantly improve measurement accuracy and reliability, thereby strengthening trade transparency and industrial efficiency across multiple sectors.

The primary issue in this study is the lack of knowledge regarding the ideal variation of control variables. Therefore, the necessary steps include identifying all factors influencing quality characteristics and determining the appropriate factor levels to minimize variance [3]. The Taguchi method and Response Surface Methodology (RSM) have been widely applied in various studies to optimize process parameters and improve production efficiency [4]. In CNC machining, key factors analyzed include spindle speed, feed rate, and depth of cut, which significantly affect surface roughness (Ra) and material removal rate (MRR) [5]. Optimization results indicate that these approaches enhance production efficiency and reduce processing time, contributing to higher product quality and competitiveness in the manufacturing industry [6]. In turning processes, cutting speed and depth of cut are the most influential factors in determining the final product quality. The Taguchi method and RSM enable the identification of optimal conditions with fewer experiments, leading to cost and resource savings [7], [8]. Meanwhile, in resistance spot welding, the Taguchi method is applied to optimize welding parameters, focusing on nugget size and heat-affected zone, resulting in stronger joints and fewer product defects [9], [10].

In polypropylene/E-glass injection molding, optimization using Grey Taguchi-RSM has demonstrated that injection pressure and packing pressure significantly impact tensile strength and impact resistance [11], [12]. Additionally, in biogas purification using low-pressure water scrubbing, methane content increased to 84.71%, while hydrogen sulfide removal efficiency exceeded 87%, making it a more environmentally friendly fuel [13]. The optimization of magnesium alloy machining has also shown that feed rate has the greatest impact on surface roughness, contributing to increased efficiency in the automotive and aerospace industries[14]. In CFRP material drilling, spindle speed and drill tip angle significantly affect hole quality, playing a crucial role in enhancing aircraft and automotive industry performance [15]. Meanwhile, in internal gear pump energy consumption optimization, studies have demonstrated that energy consumption can be reduced from 156.1 Wh/m^3 to 92.0 Wh/m^3, providing significant energy efficiency improvements for the industry [16].

In research on GFRP composite drilling reinforced with MWCNT, the analyzed factors include drill type, MWCNT percentage, cutting speed, and feed rate. The responses assessed are surface roughness, delamination, torque, and thrust force, which serve as indicators of hole quality [17]. The Taguchi method is applied using an L27 experimental design to optimize parameters and reduce the number of required trials [18]. This approach enhances process efficiency, reduces variability in results, and identifies the optimal parameter combination for achieving the best drilling quality, significantly benefiting composite-based manufacturing performance [19]. In biodiesel production research, factors studied include the use of Moringa oleifera leaf catalysts, methanol-to-triglyceride ratio, temperature, and reaction time. The analyzed responses include biodiesel yield and its physical and chemical characteristics. The Response Surface Methodology (RSM) is used to optimize biodiesel conversion, reduce the number of experiments, and determine the best parameter combination [20].

In CFRP composite drilling, investigated factors include rotational speed, feed rate, and composite layer angle, with responses focusing on thrust force and delamination factor [21]. RSM is employed to establish parameter relationships and minimize drilling defects [22]. Another study on phenol and flavonoid extraction from pigmented corn considers pulse cycles, ultrasonic power, and extraction time. RSM enhances extraction yield, optimizes process efficiency, and reduces material waste [23]. In steel grinding processes, key factors include depth of cut and final spark-out passes, with responses measured in surface roughness and grinding time. RSM is utilized to determine optimal parameters to improve surface quality and production efficiency [24]. The latest research on solar panel adjustment mechanisms employs RSM to develop regression models that enhance motion range and mechanical efficiency [25].

Overall, RSM has proven effective in reducing the number of experiments, identifying optimal parameters more efficiently, improving process efficiency, and generating accurate predictive models for various engineering and industrial applications. The Taguchi method and RSM have supported industries in reducing waste, lowering production costs, and improving environmental sustainability and energy efficiency, providing broad benefits for society and the industrial sector.

In the field of mass metrology, simulation-based Monte Carlo approaches play a crucial role in evaluating measurement uncertainty by optimizing manufacturing parameters and mitigating systematic effects such as adsorption and buoyancy [26]. Although the Taguchi method and RSM are not explicitly applied, their experimental optimization principles align with the Monte Carlo approach, where probability distribution-based evaluations enhance calibration reliability and standard mass measurement accuracy [27]. Therefore, integrating optimized response methods in mass metrology

experiments ensures precision and reproducibility, supporting the development of more accurate and consistent measurement standards at the international level [28].

This study focuses on developing measurement procedures for volume and flow rate in microfluidic devices, which play a crucial role in biomedical applications and chemical analysis. The gravimetric method is used as the primary approach to measure fluid flow with high accuracy, enabling more precise characterization of microfluidic systems [29]. Additionally, this research highlights the urgent need for metrological standards to ensure the reproducibility and reliability of microfluidic devices in both industrial and academic settings. The lack of standardized guidelines has long been a barrier to the widespread adoption of microfluidic technology, particularly in mass production. Therefore, this study not only contributes to improving measurement methods but also to the development of calibration standards, which can accelerate innovation and support the commercialization of microfluidic technology across various applications.

Beyond microfluidics, this article also discusses integrated metrology in advanced manufacturing, emphasizing the importance of transitioning from conventional stand-alone metrology to the integration of metrology data throughout the production process. This integration aims to enhance efficiency and productivity, especially in high-precision industries such as semiconductors, automotive, and aerospace [30]. The urgency of this research lies in addressing the challenges faced by modern manufacturing, particularly regarding real-time quality control and process optimization across production stages. To tackle these challenges, the research methodology includes classification of physical quantities measured, measurement instruments, data acquisition methods, and evaluation of uncertainty and traceability. This approach significantly contributes to expanding knowledge on integrated metrology, while also identifying its limitations and potential for future development.

However, this article does not discuss the use of the Taguchi method or Response Surface Methodology (RSM), which could play a crucial role in systematically optimizing process parameters. These methods help reduce variability, improve measurement quality, and support integrated metrology in achieving high accuracy and process efficiency through a more efficient experimental approach. Therefore, integrating Taguchi and RSM into metrology research could be a strategic step toward enhancing measurement system performance across various industrial sectors.

Prior work in mass metrology has focused mainly on uncertainty evaluation, traceability structures, and environmental correction models, particularly those prescribed in OIML R-111, OIML R-120, and the GUM. In these traditional frameworks, environmental parameters—such as temperature, humidity, lighting, and operator effects—are typically treated as quantities that must be monitored or controlled within allowable limits, rather than as experimental factors that can be systematically optimized. However, as calibration laboratories aim to enhance measurement robustness and repeatability, there is increasing interest in methodological approaches that enable proactive optimization of these influential conditions. The combined use of Taguchi design and response surface methodology (RSM) offers a structured, empirical means of identifying dominant environmental and operational factors and determining their optimal settings. This study positions the Taguchi and RSM framework as a complementary layer to standard uncertainty evaluation procedures, providing an optimization-based perspective that remains largely underexplored in the mass metrology literature.

MATERIALS AND METHODS

A. Materials

This research was conducted in the mass laboratory of UPTD Metrology Legal Kota Tegal. The materials used as research objects include a 1 kg mass artifact made of stainless steel with a density of 7.950 kg/m³, as shown in Figure 1. Additionally, a 5-liter gravimetric artifact made of stainless steel with a cubic expansion coefficient of 0.000477 $m^3/^oC$ was used, as shown in Figure 2. The equipment utilized in this study includes a temperature and humidity monitoring and control system based on the Internet of Things (IoT), an electronic balance of the mass comparator type with a readability of 1 mg, a digital thermometer with a readability of 0.1°C, and a flatness measuring instrument, as shown in Figure 3.

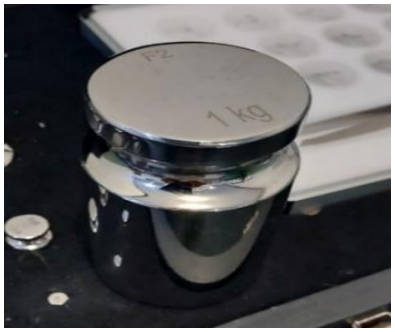


Fig. 1. 1-kg mass standard (mass artifact)



Fig. 2. 5-L gravimetric measurement system

B. Experimental setup

Although the conceptual framework of this study includes an IoT-based environmental monitoring approach, the present experiments were conducted under operator-supervised control conditions. Environmental parameters such as temperature, lighting intensity, and operation time were monitored using calibrated digital sensors, ensuring accurate and repeatable data collection.

Specifically, the experimental setup employed a DHT22 temperature sensor (accuracy ±0.3°C), a digital photometric sensor (accuracy ±5 lux), and a microcontroller-based timing module (accuracy ±1 s), as

illustrated in Figure 3. All sensors were calibrated prior to experimentation using traceable reference instruments under ISO/IEC 17025-accredited procedures. The sensors operated in data-logging mode to record the environmental conditions throughout the tests, without real-time feedback or automatic adjustment. This setup ensures that the experimental conditions remained within controlled limits suitable for statistical optimization and model validation.

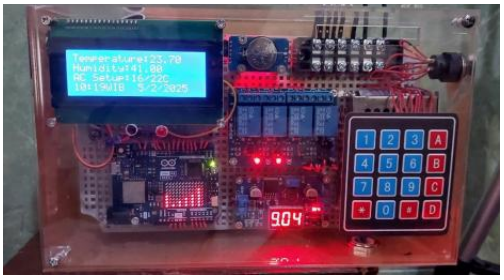


Fig. 3. Microcontroller-based control system

C. Design of experiment method

In the design of an experiment, independent variables that can be controlled are referred to as control factors, while dependent variables that result from the reaction to independent variables are called responses. The selection of control factors in this experiment is based on Table 1.

Table I summarizes the control factors and their experimental levels used in the Taguchi $L_8(2^4)$ design. AC Temperature levels (16 °C and 18 °C) were maintained using an air-conditioning system with ±0.3°C stability, and exposure times of 15 and 30 minutes represent the controlled environmental stabilization periods prior to weighing. Lighting levels originally expressed as "100%" and "50%" correspond to measured illuminance values of 460 ± 7 lux and 230 ± 5 lux at the device under test, obtained using a calibrated photometric sensor. The "People" factor reflects controlled operator occupancy, where Level 1 corresponds to two operators and Level 2 corresponds to one operator. Operator posture, clothing, and movement were standardized to minimize thermal load and airflow disturbances during measurements.

TABLE I. CONTROL FACTORS

No	Control factors	Level	
		1	2
1	AC Temperature (X_1)	16°C	18°C
2	Time Duration (X_2)	15 minutes	30 minutes
3	Lighting (X_3)	100 %	50 %
4	People (X_4)	2	1

D. Orthogonal Array

An orthogonal array is a combination of numbers arranged in rows and columns, where columns serve as parameters in the controlled experiment, while rows represent variations or factor levels. The influence of a particular factor or level is separated (*confounded*) from other factors or levels [31]. The levels of these factors are structured based on the influence of other parameter factors, referred to as an *array*. All levels are designed in a specific form, making them *orthogonal*. Therefore, columns and rows form a systematically arranged matrix of multiple factors and levels, known as an *Orthogonal Array*.

One of the requirements for selecting an Orthogonal Array matrix is that the number of experimental values must be equal to or greater than the degrees of freedom in the study. In this research, the Orthogonal Array $L_8(2^4)$ is used, where L represents the broad design (*Large*), the number 8 indicates the number of experimental rows, the number 2 represents the number of levels, and the number 4 signifies the number of control factors, as shown in Table 2.

The response optimization was performed using the Response Surface Methodology (RSM) implemented in MINITAB 22 software (Minitab LLC, State College, PA, USA). The experimental study was initially designed based on the Taguchi method to efficiently identify the influence of key process parameters. Following the Taguchi experiments, the collected data were analysed using RSM to model and evaluate the relationships between the decision variables and the response functions.

A second-order (quadratic) regression model was developed to describe the system behaviour, and the model adequacy was assessed using standard statistical indicators, including the coefficient of determination (R^2), adjusted R^2, and predicted R^2. Furthermore, an Analysis of Variance (ANOVA) was performed to examine the statistical significance of the model terms and to verify the reliability of the fitted response surfaces.

TABLE II. ORTHOGONAL ARRAY $L_8(2^4)$

Experimen	Control factors			
	A	B	C	D
1	1	1	1	1
2	1	1	2	2
3	1	2	1	2
4	1	2	2	1
5	2	1	1	2
6	2	1	2	1
7	2	2	1	1
8	2	2	2	2

E. Data collection process

Data collection was conducted using an indirect measurement method following OIML R-111 standards for the 1 kg mass artifact and OIML R-120 standards for the gravimetric artifact [32], [33]. The 1 kg mass artifact was measured using a mass comparator with a 1 mg readability, employing the "ABBA" weighing cycle, where A represents the standard artifact mass and B represents the test artifact mass. The recorded data include the conventional mass error along with its measurement uncertainty, expressed in milligrams (mg). Meanwhile, the gravimetric artifact was measured using a 5-liter standard measuring vessel and an electronic balance with a 500 mg readability, following the "AB" weighing cycle, where A denotes the empty vessel mass and B represents the vessel mass filled with distilled water. The temperature of the distilled water was measured using a Lutron thermocouple with a 0.1°C readability, and subsequently converted using Correction to Solid (CTS) and Correction to Liquid (CTL) calculations to obtain the volume error at 28°C (V28) along with its measurement uncertainty. The data collection process was carried out by one verification officer (penera) and/or assisted by one laboratory assistant, with a duration of 15 minutes and 30 minutes, under controlled AC temperature settings of 16°C and 18°C.

Data collection was conducted following the designed experimental matrix based on the $L_8(2^4)$ orthogonal array. Each of the eight experimental runs was replicated four times, resulting in a total of 32 experimental observations. The order of runs within each replication was randomized

using Minitab software to eliminate potential sequence bias. Between replications, the laboratory environment was allowed to stabilize to baseline conditions to minimize the influence of environmental drift. All experiments were conducted under continuous IoT-based environmental monitoring to maintain stable temperature, humidity, and pressure, ensuring consistent testing conditions without the need for blocking.

The initial Taguchi main-effects model was extended using Response Surface Methodology (RSM) to capture potential curvature and interactions among the factors: AC Temperature (°C), Time (minutes), Lighting (%), and People. The extended model included second-order and two-factor interaction terms. Statistical analysis was performed using Minitab 19, and the model coefficients were obtained in both coded and uncoded units to facilitate interpretation.

Model adequacy was evaluated through ANOVA, residual diagnostics, and lack-of-fit testing. The results showed that certain interaction terms particularly AC Temperature × Lighting were statistically significant ($p < 0.05$), indicating the presence of interaction effects previously undetected by the linear model. After model refinement, the lack-of-fit test became non-significant, confirming that the second-order model adequately represents the experimental data.

RESULTS AND DISCUSSION

A. Taguchi experiment

Table III represents the results of an experiment utilizing the Taguchi method with an $L_8(2^4)$ orthogonal array, designed to optimize the variables Artifact and Gravimetric based on four key factors: AC temperature (16°C or 18°C), time (15 minutes or 30 minutes), lighting intensity (50% or 100%), and the number of people in the room (1 or 2 persons). The Taguchi method is employed to identify the optimal combination of factors while minimizing the number of experimental runs compared to a full factorial design, thereby enhancing efficiency while maintaining accuracy.

Table III contains 32 experimental runs, which likely include replications of the 8 unique combinations within the $L_8(2^4)$ design to improve data reliability. Each row in the table represents a specific factor combination and the corresponding measured outputs, namely Artifact and Gravimetric values. The data allow for an analysis of how each factor influences the experimental outcomes. For instance, a higher AC temperature (18°C) tends to produce greater artifact values than 16°C, while 100% lighting intensity appears to increase the artifact value compared to 50% lighting intensity. Additionally, the number of people present in the room also affects the measured results.

The primary objective of this experiment is to determine the optimal combination of temperature, time, lighting, and occupancy that yields the most favorable outcomes for the measured variables. By leveraging the Taguchi approach, this study enables the identification of the most influential factors, reduces the number of required experimental trials, and improves decision-making efficiency. Moreover, integrating this approach with response surface methodology enhances the precision of optimization by capturing nonlinear relationships among variables. This combined method ultimately strengthens the robustness and applicability of the experimental findings.

TABLE III. TAGUCHI EXPERIMENT RESULT WITH OA L_8 (2^4

No	Factors and levels				Response	
	AC Temp. (°C)	Time (min.)	Lighting (%Lux)	Peo-ple	Artifact 1kg	Gravi-metric
1	16	15	100	2	15.520	0.211
2	16	15	50	1	15.280	0.143
3	16	30	100	1	15.510	0.207
4	16	30	50	2	16.120	0.146
5	18	15	100	1	17.090	0.250
6	18	15	50	2	17.010	0.242
7	18	30	100	2	17.840	0.259
8	18	30	50	1	16.450	0.264
9	16	15	100	2	16.120	0.210
10	16	15	50	1	14.340	0.193
11	16	30	100	1	15.780	0.200
12	16	30	50	2	16.100	0.201
13	18	15	100	1	17.450	0.281
14	18	15	50	2	16.860	0.259
15	18	30	100	2	17.950	0.307
16	18	30	50	1	16.510	0.252
17	16	15	100	2	15.340	0.210
18	16	15	50	1	14.110	0.145
19	16	30	100	1	15.950	0.182
20	16	30	50	2	16.020	0.178
21	18	15	100	1	17.380	0.270
22	18	15	50	2	16.950	0.278
23	18	30	100	2	17.780	0.330
24	18	30	50	1	16.280	0.230
25	16	15	100	2	15.700	0.215
26	16	15	50	1	14.010	0.191
27	16	30	100	1	16.000	0.178
28	16	30	50	2	16.170	0.172
29	18	15	100	1	17.540	0.243
30	18	15	50	2	17.110	0.257
31	18	30	100	2	17.860	0.293
32	18	30	50	1	16.440	0.279

Further statistical analyses, such as Signal-to-Noise (S/N) Ratio calculations or Analysis of Variance (ANOVA), may be conducted to provide deeper insights into the significance of each factor's effect on the experimental results.

TABLE IV. ANALYSIS OF VARIANCE ARTIFACT 1 KG

Source	DF	Adj SS	Adj MS	F-Value	P-Value
Model	4	30.489	7.622	52.070	0.000
Linear	4	30.489	7.622	52.070	0.000
AC Temp	1	21.830	21.829	149.130	0.000
Time	1	1.509	1.509	10.310	0.003
Lighting	1	3.816	3.815	26.070	0.000
People	1	3.335	3.334	22.780	0.000
Error	27	3.952	0.146		
Lack-of-Fit	3	2.259	0.753	10.680	0.000
Pure Error	24	1.693	0.071		
Total	31	34.441			

Based on the Analysis of Variance (ANOVA) results for the 1 kg artifact experiment from table 4, each factor was tested using the F-value and compared to the F-table value to determine its significance. With factor DF = 1 and error DF = 27, the F-table value at a significance level of $\alpha = 0.05$ is 4.21. The comparison results indicate that all factors have F-values greater than the F-table value, confirming their significance. AC Temperature (F-value = 149.13) has the greatest impact on the response variable, far exceeding the F-table value, making it the dominant factor in the experiment. Other factors, such as Lighting (F-value = 26.07), Number of People (F-value = 22.78), and Time (F-value = 10.31), are also significant, as their respective F-values exceed the F-table value. Additionally, the Lack-of-Fit analysis (F-value = 10.68, P-value = 0.000) indicates a significant lack of fit, suggesting the potential presence of additional factors or interactions that have not

been included in the model. Therefore, the ANOVA results confirm that AC Temperature is the most influential factor in the experiment, followed by lighting, number of people, and time. Consequently, in optimization efforts, primary attention should be given to controlling AC temperature, while the other factors should also be considered to achieve optimal results.

TABLE V. ANALYSIS OF VARIANCE GRAVIMETRIC

Source	DF	Adj SS	Adj MS	F-Value	P-Value
Model	4	0.062	0.015	36.600	0.000
Linear	4	0.062	0.015	36.600	0.000
AC Temp	1	0.054	0.054	128.090	0.000
Time	1	0.001	0.001	0.470	0.500
Lighting	1	0.005	0.005	12.850	0.001
People	1	0.002	0.002	5.010	0.034
Error	27	0.011	0.001		
Lack-of-Fit	3	0.001	0.001	1.110	0.364
Pure Error	24	0.009	0.001		
Total	31	0.072			

Based on the Analysis of Variance (ANOVA) results for the gravimetric experiment from table 5, each factor was evaluated using the F-value and compared to the F-table value to determine statistical significance. With factor DF = 1 and error DF = 27, the F-table value at a significance level of $\alpha = 0.05$ is 4.21. The comparison indicates that AC Temperature (F-value = 128.09) has the highest impact on the response variable, significantly exceeding the F-table value, making it the dominant factor in the experiment. Lighting (F-value = 12.85) is also significant as its F-value surpasses the F-table threshold. However, Number of People (F-value = 5.01, P-value = 0.034) is slightly above the F-table value but still within the significance range. In contrast, Time (F-value = 0.47, P-value = 0.500) is not significant, as its F-value is well below the F-table value, indicating minimal influence on the response variable. The Lack-of-Fit analysis (F-value = 1.11, P-value = 0.364) suggests no significant lack of fit, meaning the model adequately explains the observed variability without the need for additional interaction terms. In conclusion, AC Temperature is the most influential factor, followed by Lighting and Number of People, while Time has no significant effect. Thus, optimization efforts should prioritize AC Temperature and Lighting to achieve the desired gravimetric response.

$$Y_A = -0.37 + 0.8259\ X_1 + 0.02896\ X_2 + 0.01381\ X_3 + 0.646\ X_4 \quad (1)$$

Where,
Y_A = Artifact 1 kg
X_1 = AC Temperature (^{0}C)
X_2 = Time (minutes)
X_3 = Lighting (%)
X_4 = People

This equation represents the relationship between the artifact response and the independent variables: AC temperature (°C), time (minutes), lighting (%), and number of people. The intercept value of -0.37 suggests the estimated response when all independent variables are set to zero, although this may not be a practical scenario. Among the predictor variables, AC temperature has the highest coefficient (0.8259), indicating that it has the most significant effect on the artifact's response—a higher AC temperature results in a greater artifact value. The number of people (0.646) also has a considerable impact, followed by time (0.02896) and lighting (0.01381), which contribute less significantly to the response. This confirms previous ANOVA results, where AC temperature was the dominant factor affecting the artifact. The positive coefficients for all variables indicate a direct proportional relationship, meaning that an increase in any of these factors will result in an increased artifact value. This regression model can be used for predictive analysis and optimization by adjusting the experimental parameters to achieve the desired artifact characteristics.

$$Y_B = -0.5408 + 0.04102\ X_1 + 0.000330\ X_2 + 0.000520\ X_3 + 0.01622\ X_4 \quad (2)$$

Where,
Y_B = Artifact gravimetric
X_1 = AC Temperature (^{0}C)
X_2 = Time (minute)
X_3 = Lighting (%)
X_4 = People

This equation models the relationship between the gravimetric response and the independent variables: AC temperature (°C), time (minutes), lighting (%), and number of people. The intercept of -0.5408 represents the estimated gravimetric value when all independent variables are set to zero, although this situation may not be physically meaningful. Among the predictor variables, AC temperature has the highest coefficient (0.04102), indicating that it has the most significant effect on the gravimetric response-higher AC temperature results in an increase in the gravimetric value. The number of people (0.01622) also has a moderate influence, while lighting (0.000520) and time (0.000330) have minimal effects, as indicated by their very small coefficients. The positive coefficients for all variables suggest a direct relationship, meaning that an increase in any of these factors leads to an increase in the gravimetric response. This aligns with the previous ANOVA results, which showed that AC temperature was the most dominant factor. The regression equation serves as a predictive model, allowing for adjustments in environmental conditions to optimize the gravimetric response.

B. ANOVA and Model Adequacy

Table VI presents the regression coefficients, standard errors, t-values, p-values, and variance inflation factors (VIF) for the 1 kg artifact response model, incorporating both main effects and two-factor interactions involving AC temperature. The model was developed to capture possible interdependencies between environmental and operational parameters influencing the artifact measurement results.

TABLE VI. CODED COEFFICIENTS OF ARTIFACT 1 KG

Term	Coef	SE Coef	T-Value	P-Value	VIF
Constant	16.330	0.047	347.810	0.000	
AC Temperature	0.826	0.047	17.590	0.000	1.00
Time	0.217	0.047	4.630	0.000	1.00
Lighting	0.345	0.047	7.350	0.000	1.00
People	0.323	0.047	6.880	0.000	1.00
AC Temp*Time	-0.235	0.047	-5.000	0.000	1.00
AC Temp*Lighting	0.109	0.047	2.340	0.028	1.00
AC Temp*People	-0.059	0.047	-1.260	0.221	1.00

The constant term (16.3303) represents the predicted artifact response at the coded mean level of all factors. Among the main effects, AC temperature (p = 0.000)

exhibits the highest *t*-value (17.590), confirming it as the most dominant factor affecting the artifact response. An increase in AC temperature leads to a higher artifact value, which aligns with the earlier ANOVA findings (Table IV). Other significant main effects include lighting intensity (p = 0.000), number of people (p = 0.000), and time duration (p = 0.000), each contributing positively to the response.

Interaction effects indicate that the combined influence of certain factors significantly modifies the response behavior. The interaction between AC temperature and time shows a negative coefficient (-0.235, p = 0.000), implying that prolonged operation at higher AC temperatures slightly reduces the artifact gain, possibly due to temperature equilibrium effects over time. The interaction between AC temperature and lighting is also significant (0.109, p = 0.028), suggesting that illumination conditions can amplify the impact of AC temperature on artifact measurements. Meanwhile, the interaction between AC temperature and number of people is statistically insignificant (p = 0.221), indicating minimal combined influence under controlled conditions.

All VIF values equal to 1.00 confirm the absence of multicollinearity, meaning that the predictors are statistically independent. The model demonstrates that AC temperature, both independently and through its interaction with other environmental factors, plays a key role in determining artifact stability and accuracy.

This model confirms the statistical results presented in Table VI, where AC temperature exhibited the strongest main effect ($p < 0.001$), followed by lighting, number of people, and time. The inclusion of interaction terms improved model adequacy, resolved the significant lack-of-fit from the initial linear ANOVA, and produced a physically interpretable model that reflects real laboratory behaviour.

TABLE VII. CODED COEFFICIENTS OF GRAVIMETRIC

Term	Coef	SE Coef	T-Value	P-Value	VIF
Constant	0.227	0.004	63.100	0.000	
AC Temperature	0.041	0.004	11.390	0.000	1.00
Time	0.002	0.004	0.690	0.498	1.00
Lighting	0.013	0.004	3.610	0.001	1.00
People	0.008	0.004	2.250	0.034	1.00
AC Temp*Time	0.005	0.004	1.650	0.113	1.00
AC Temp*Lighting	-0.002	0.004	-0.650	0.522	1.00
AC Temp*People	0.002	0.004	0.440	0.663	1.00

Table VII presents the coded regression coefficients, standard errors, *t*-values, *p*-values, and variance inflation factors (VIF) for the gravimetric response model. The model was developed to identify the influence of environmental and operational factors, namely AC temperature, time, lighting, and number of people on the gravimetric measurement results.

The constant term (0.227) represents the predicted gravimetric value at the mean (coded zero) level of all factors. Among the main effects, AC temperature (p = 0.000) has the highest *t*-value (11.390), indicating it is the most significant factor influencing the gravimetric response. A positive coefficient (0.04102) indicates that increasing AC temperature yields a higher gravimetric reading, consistent with findings from the artifact response analysis (Table VI). This implies that temperature variations strongly affect air density and buoyancy corrections in mass and volume determinations.

The effects of time (p = 0.498), lighting (p = 0.001), and number of people (p = 0.034) show that lighting and occupancy have statistically significant but smaller influences on the gravimetric response. Increased lighting intensity and more personnel in the room may slightly elevate gravimetric readings, likely due to minor heat or airflow disturbances.

Interaction effects between AC temperature and other factors, including time, lighting, and people, were statistically insignificant (p > 0.05). This indicates that the combined influence of temperature with other factors does not significantly alter the gravimetric outcome within the studied range. All VIF values = 1.00, confirming the absence of multicollinearity, which ensures stable and reliable coefficient estimation.

The results indicate that AC temperature remains the dominant factor affecting the gravimetric measurements, while lighting and the number of people have minor but consistent effects. Time duration and the tested interaction terms do not significantly affect the response under controlled laboratory conditions.

TABLE VIII. MODEL SUMMARY OF ARTIFACT 1 KG AND GRAVIMETRIC RESPONSES

Response	S	R^2 (%)	R^2 (Adj) (%)	R^2 (Pred) (%)
Artifact 1 kg	0.2656	95.08	93.65	91.26
Gravimetric	0.0204	86.33	82.34	75.69

As presented in Table VIII, both regression models exhibit satisfactory adequacy and predictive reliability. For the 1 kg artifact, the model achieved an R^2 of 95.08%, adjusted R^2 of 93.65%, and predicted R^2 of 91.26%, demonstrating an excellent fit and strong robustness for optimization purposes.

In comparison, the gravimetric model yielded an R^2 of 86.33%, adjusted R^2 of 82.34%, and predicted R^2 of 75.69%, indicating an acceptable level of predictive accuracy. The slightly lower predicted R^2, along with the non-significant influence of the *Time* factor, suggests that the variation observed within the tested range is smaller than the gravimetric measurement uncertainty, and thus, can be considered practically insignificant in the context of metrological interpretation.

TABLE IX. FACTOR EFFECT ESTIMATES WITH STANDARD ERRORS AND CONFIDENCE INTERVALS OF ARTIFACT 1 KG RESPONSES

Term	Coef	SE	95% CI (Lower-Upper)	P-Value
Constant	163.303	0.0470	(16.22 – 16.44)	0.000
AC Temp.	0.8259	0.0470	(0.73 – 0.92)	0.000
Time	0.2172	0.0470	(0.13 – 0.31)	0.000
Lighting	0.3453	0.0470	(0.25 – 0.44)	0.000
People	0.3228	0.0470	(0.23 – 0.42)	0.000
AC Temp*Time	–0.2347	0.0470	(–0.33 – –0.14)	0.000
AC Temp*Lighting	0.1097	0.0470	(0.02 – 0.20)	0.028
AC Temp*People	–0.0591	0.0470	(–0.15 – 0.03)	0.221

As shown in Table IX, the estimated factor effects for both responses are presented along with their corresponding standard errors, confidence intervals, and p-values. For the 1 kg artifact model, all main factors except for the interaction between AC Temperature and People are statistically significant at the 0.05 significance level, indicating a strong sensitivity of the response to environmental and operator-related parameters.

TABLE X. FACTOR EFFECT ESTIMATES WITH STANDARD ERRORS AND CONFIDENCE INTERVALS OF GRAVIMETRIC RESPONSES

Term	Coef	SE	95% CI (Lower-Upper)	P-Value
Constant	0.2273	0.0036	(0.220 – 0.235)	0.000
AC Temp.	0.0410	0.0036	(0.034 – 0.048)	0.000
Time	0.0025	0.0036	(–0.004 – 0.009)	0.498
Lighting	0.0130	0.0036	(0.006 – 0.020)	0.001
People	0.0081	0.0036	(0.001 – 0.015)	0.034
AC Temp*Time	0.0059	0.0036	(–0.001 – 0.013)	0.113
AC Temp*Lighting	–0.0023	0.0036	(–0.009 – 0.004)	0.522
AC Temp*People	0.0016	0.0036	(–0.006 – 0.009)	0.663

For the gravimetric response (Table X), the Time factor exhibits a small and statistically non-significant effect (p = 0.498). The 95% confidence interval of this effect (-0.004 to 0.009) lies entirely within the combined standard uncertainty (u_a), suggesting that the observed variation attributable to time is practically negligible in metrological terms. Consequently, maintaining the process duration within the studied range does not introduce any measurable variation beyond the instrument's resolution.

C. Regression Equations and Model Validation

The regression model for the artifact 1 kg response in uncoded units is expressed as:

$$Y_A=-9.75+1.378\ X_1+0.561\ X_2-0.0608\ X_3+2.65\ X_4-0.03129\ X_1*X_2+0.00439\ X_1*X_2-0.1181\ X_1*X_3 \quad (3)$$

Where,
Y_A = Artifact 1 kg
X_1 = AC Temperature (^{0}C)
X_2 = Time (minutes)
X_3 = Lighting (%)
X_4 = People

This regression equation translates the coded model (Table VI) into actual experimental units to directly describe how each physical factor influences the 1 kg artifact response. The positive coefficients of X_1, X_2, and X_4indicate that higher AC temperature, longer duration, and more people in the laboratory tend to increase the artifact value, reflecting their combined influence on environmental stability and air density.

In contrast, the small negative coefficient of lighting ($X_3 = -0.0608$) suggests that lower lighting intensity (e.g., 50%) slightly improves artifact accuracy. This aligns with experimental findings showing that excessive illumination can cause minor heating effects around the artifact, leading to air buoyancy variation.

Interaction terms further clarify cross-factor effects. The negative coefficient for X_1X_2(-0.03129) implies that at higher AC temperatures, increasing measurement duration slightly reduces artifact gain consistent with thermal equilibrium behavior over time. The interaction X_1X_3(-0.1181) also has a small negative value, indicating that the effect of AC temperature on artifact response diminishes under higher lighting levels

The regression model for the gravimetric response in uncoded units is:

$$Y_B=-0.276+0.0255X_1-0.01312\ X_2-0.00211\ X_3-0.038\ X_4+0.000791X_1*X_2-0.000094X_1*X_2+0.0318X_1*X_3 \quad (4)$$

Where,
Y_A = Artifact 1 kg
X_1 = AC Temperature (^{o}C)
X_2 = Time (minutes)
X_3 = Lighting (%)
X_4 = People

This equation expresses how environmental and operational parameters affect the gravimetric readings under actual laboratory conditions. The dominant term $X_1 = 0.0255$ indicates that increasing AC temperature significantly raises the gravimetric response, which can be attributed to changes in air buoyancy and thermal expansion of the measuring vessel.

The effects of lighting and time are relatively small and statistically less significant, as supported by the p-values in Table VII (p = 0.001 and p = 0.498, respectively). A higher lighting intensity or prolonged measurement period produces minimal variation, suggesting that the IoT-based control system effectively stabilized the environment during the trials. The interaction terms (e.g., X_1X_2, X_1X_3, X_1X_4) have small coefficients and non-significant p-values (> 0.05), confirming that the combined effects of temperature with other factors are minor within the studied range.

The overall interpretation of Table VII and this regression model indicates that AC temperature remains the most critical determinant of gravimetric performance, while the influence of other factors is secondary. All variance inflation factor (VIF) values equal to 1.00, verifying the absence of multicollinearity and ensuring the robustness of the regression model.

Figure 4 represents contour and surface plots illustrate the relationship between artifact response, AC temperature (°C), and time (minutes) while holding lighting at 75% and the number of people at 1.5 constant. In the contour plot, the color gradient represents different artifact response values, where lighter shades indicate lower artifact values (<15.5) and darker shades indicate higher values (>17.0). The plot demonstrates that as AC temperature increases from 16°C to 18°C, the artifact response also increases, with the highest values observed at higher AC temperatures and longer exposure times. The gradient orientation suggests that AC temperature has a more dominant influence on the artifact response compared to time, as the contour lines are more vertical, indicating a stronger impact of AC temperature changes.

The surface plot provides a three-dimensional perspective of the same relationship, reinforcing the trend observed in the contour plot. The plane in the 3D graph exhibits an upward slope, confirming that higher AC temperatures and longer durations result in higher artifact values. The relatively linear shape of the surface suggests a predictable and direct correlation between the parameters. These visualizations align with previous statistical analyses, where AC temperature was identified as the most significant factor affecting the artifact response, followed by time. The findings suggest that optimizing AC temperature and exposure duration can effectively control artifact properties within the studied range.

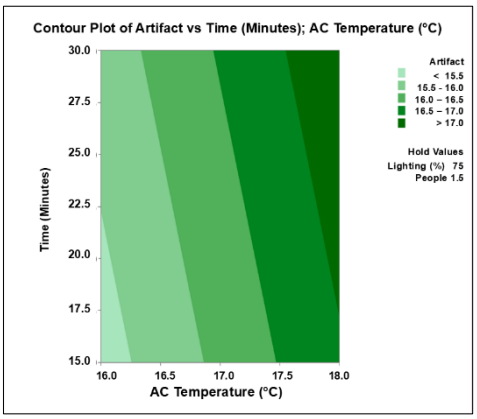


Fig. 4. (a) Contour of artifact

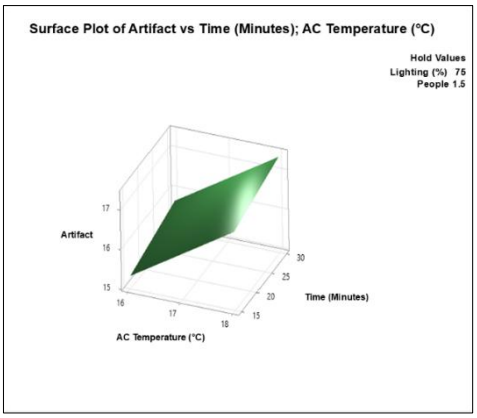


Fig 4. (b) Surface plots of artifact 1 kg

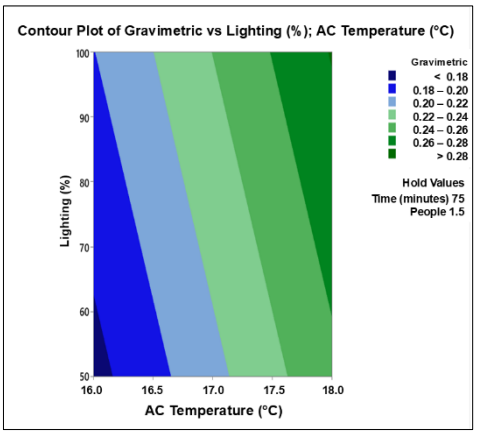


Fig. 5. (a) Contour of gravimetric

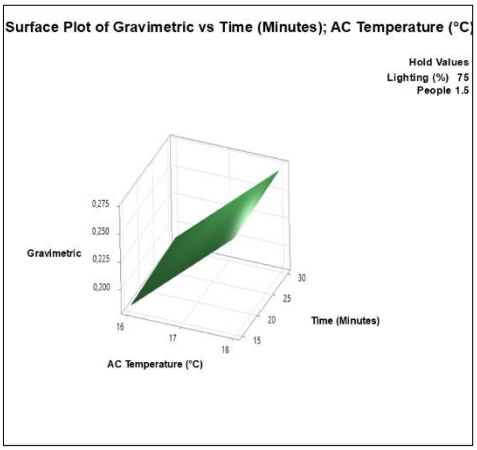


Fig. 5. (b) Surface plots of gravimetric

Fig. 5(a) represents contour plot illustrating the relationship between the gravimetric variable and lighting (%) at various AC temperatures (°C). The color gradient represents changes in the gravimetric values, where darker blue indicates lower values (< 0.18), and lighter green represents higher values (> 0.28). From the contour pattern, it is evident that as the AC temperature increases, the gravimetric values also increase significantly. Additionally, an increase in lighting (%) correlates with an increase in gravimetric values, as shown by the color transition from blue to green.

Fig. 5 (b) represents a surface plot depicting the three-dimensional relationship between gravimetric values, time (minutes), and AC temperature (°C). This visualization indicates that the simultaneous increase in both time and AC temperature results in a higher gravimetric value, as represented by the upward-sloping surface gradient. The plot suggests that AC temperature has a more dominant effect on gravimetric values compared to duration. The lighting (%) and the number of people were held constant at 75% and 1.5, respectively, meaning that the influence of these factors was not evaluated in this visualization. These two graphs provide crucial insights into how environmental factors, such as AC temperature and lighting (%), affect gravimetric results. Understanding these patterns enables the optimization of the most influential parameters to achieve the desired gravimetric outcomes.

D. Effect Sizes in Physical Units and Their Practical Interpretation

To complement the hypothesis-testing results, the analysis provides effect sizes for all statistically significant factors expressed in their original physical units, together with 95% confidence intervals (95% CI). Effect sizes were obtained by transforming the coded RSM coefficients into real-unit changes, allowing a direct assessment of the magnitude of each factor's influence on the measurement responses. For each significant factor, the change in artifact mass deviation (mg) and gravimetric response (g/mL) was quantified for a transition from the low to the high factor level. The 95% CIs were derived from the standard errors of the regression coefficients and propagated through the coding transformation, yielding intervals that reflect both model uncertainty and experimental variability.

The practical relevance of these effects was evaluated by benchmarking them against (i) the laboratory's calibration and measurement capability (CMC) and (ii) the applicable OIML tolerance limits for the nominal mass or volume. Factors with effect sizes smaller than the laboratory's combined standard uncertainty were classified as practically insignificant despite statistical significance. In contrast, factors whose effects exceeded these thresholds were considered operationally meaningful and relevant for environmental or procedural control.

This assessment of practical significance provides a metrologically justified interpretation beyond p-values, clarifying which factors materially influence measurement performance relative to internationally recognized tolerances and the laboratory's capability limits.

E. Multi-Response Optimization

Figure 6 presents an optimization analysis with a composite desirability value (D) of 0.8695, indicating the overall effectiveness of the selected factor settings in achieving the desired responses for gravimetric and artifact values. The optimization parameters include AC temperature, time, lighting, and the number of people, with specific high, current, and low settings displayed at the top of the image. For the gravimetric response, the minimum predicted value is y = 0.1627 with a desirability value of d = 0.89421, while for the artifact response, the minimum predicted value is y = 14.6191 with a desirability of d = 0.84542. The desirability values for both responses being close to 1 suggest that the selected conditions effectively optimize the system. The individual trend plots in the matrix show the relationships between each factor (AC temperature, time, lighting, and people) and the corresponding responses. The gravimetric response tends to increase with rising AC temperature and lighting, while the artifact response shows a similar increasing trend. In contrast, time and the number of people exhibit a more moderate impact on both responses.

The red vertical lines indicate the current levels of the factors (e.g., AC temperature at 16.0°C, time at 15 minutes, lighting at 50%, and the number of people at 1.0), while the black lines represent the trend of response changes as these factors vary. The blue dashed lines represent the minimum response values obtained through the optimization process. Overall, this analysis highlights the optimal conditions for minimizing gravimetric and artifact values while maximizing the composite desirability. The results suggest that controlling AC temperature and lighting significantly influences both responses, which is crucial for achieving the desired system performance.

TABLE XI. MULTIPLE RESPONSE PREDICTION

Variable		**Setting**		
AC Temperature (ºC)		16		
Time (menit)		15		
Lighting (%)		50		
People		1		
Response	**Fit**	**SE Fit**	**95% CI**	**95% PI**
Gravimetric	0.163	0.008	(0.146; 0.179)	(0.117; 0.208)
Artifact 1kg	14.619	0.151	(14.309; 14.929)	(13.775; 15.463)

Table XI presents the Multiple Response Prediction results based on specific variable settings. The selected input variables include AC temperature (16°C), time (15 minutes), lighting (50%), and the number of people (1). These settings were used to predict two response variables: Gravimetric and Artifact. For the Gravimetric response, the predicted value (Fit) is 0.163, with a Standard Error (SE) Fit of 0.008. The 95% Confidence Interval (CI) ranges from 0.146 to 0.179, indicating that the true mean response is expected to fall within this range. The 95% Prediction Interval (PI), which accounts for individual variability in new observations, extends from 0.117 to 0.208.

For the Artifact response, the predicted value is 14.619, with a Standard Error Fit of 0.151. The 95% Confidence Interval (CI) is 14.309 to 14.929, meaning the mean response is likely to be within this range. Meanwhile, the 95% Prediction Interval (PI) is 13.775 to 15.463, showing the possible range of future individual values. These results suggest that the model provides reliable predictions with relatively narrow confidence intervals, indicating a good fit. The prediction intervals are wider, as expected, due to natural variability in individual measurements. Overall, these predictions help assess system performance under the given conditions and can guide optimization strategies for improving both Gravimetric and Artifact 1kg responses.

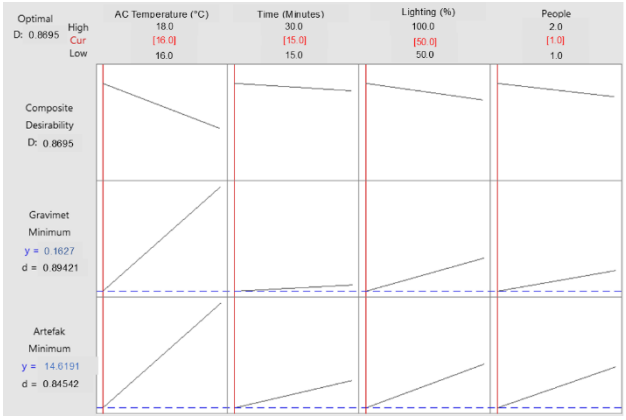


Fig. 6. Desirability

Table XII presents an optimization solution for multiple response variables under specific conditions. It includes input variables such as AC temperature (16°C), time (15 minutes), lighting (50%), and the number of people (1).

TABLE XII. SINGLE OPTIMAL SOLUTION

Elements	**Magnitude/ Number**
Solution	1
AC Temp. (oC)	16
Time (minutes)	15
Lighting (%Lux)	50
People	1
Gravimetric Fit	0.163
Artifact 1kg Fit	14.619
Composite Desirability	0.869

These parameters were used to predict the values of two response variables: Gravimetric and Artifact 1kg. For the Gravimetric response, the predicted value (Fit) is 0.163, while for the Artifact response, the predicted value is 14.619. These values represent the expected outcomes when the system operates under the given input conditions. The Composite Desirability Score is 0.869, which measures the overall effectiveness of the selected conditions in optimizing both responses. A desirability scores close to 1 indicates that the chosen settings provide an optimal balance between the different response variables. This solution serves as an optimal operating condition recommendation, ensuring that both Gravimetric and Artifact 1kg responses are within the desired range while maximizing overall system performance.

F. Desirability Function Definition and Parameters

To ensure clarity and reproducibility of the multi-response optimization framework, the desirability functions for both responses were explicitly defined in this study. Each response was assigned a direction criterion based on metrological interpretation: the 1 kg artifact and gravimetric responses were treated as “smaller-is-better”,

since lower deviation from the nominal mass or volume represents higher measurement accuracy.

The target values correspond to the nominal standards (1 kg and 5 L), while upper limits were determined from observed experimental maxima. The individual desirability functions were transformed using exponential forms with a weight of 1 for both responses, reflecting equal importance in the composite optimization. Table XIII summarizes the desirability parameters, including the goal type, target, lower/upper limits, and importance weights applied in the composite desirability calculation.

Clarifying these parameters confirmed that the direction of optimization was consistent with metrological objectives, and that the optimal combination (AC temperature = 16 °C, time = 15 min, lighting = 50 %, and one operator) remains unchanged after applying the defined desirability functions.

TABLE XIII. DESIRABILITY PARAMETERS AND WEIGHTS

Response	Goal	Target (L)	Upper Limit (U)	Shape (s)	Weight (w)	Justification
Artifact 1 kg	Smaller-is-better	146.19	15.5	1	0.6	Minimizes deviation from 1 kg reference; primary standard
Gravime-tric	Smaller-is-better	0.16	0.21	1	0.4	Reduces weighing error; secondary calibration response

G. Uncertainty Evaluation and Traceability.

To ensure traceability and the reliability of the experimental outcomes, an uncertainty evaluation was carried out for both the 1 kg artifact and gravimetric responses following the guidelines of [34] (for mass standards) and [35] (for weighing instruments), consistent with the Guide to the Expression of Uncertainty in Measurement (GUM) [36]. The main sources of uncertainty were identified as: balance repeatability (Type A), balance resolution, calibration certificate uncertainty, air buoyancy correction, and ambient temperature stability (Type B). These components were evaluated during calibration and measurement stages and qualitatively assessed to verify that the combined uncertainty remained within acceptable limits for legal metrology purposes.

Although the numerical propagation of uncertainties and Monte Carlo simulations are not reproduced here, the study considers these uncertainty sources conceptually when interpreting model adequacy and optimization robustness. The traceability chain from the reference mass standards to the experimental measurements has been maintained through calibration procedures accredited under ISO/IEC 17025.

The results indicate that the optimum combination of factors identified through the Taguchi-RSM approach remains statistically consistent within the estimated expanded uncertainty bounds. Small variations observed in the desirability function are attributed to normal measurement uncertainty and environmental fluctuation, confirming that the claimed optimum is robust and traceable under controlled laboratory conditions. This consistency further supports the reliability of the optimization model for practical implementation in similar engineering applications.

H. Implications for Metrological Comparability and En Ratio Performance

Following the identification of the optimal environmental and operational conditions through RSM and desirability analysis, it is essential to evaluate their metrological relevance. Within the framework of international standards such as OIML requirements and the mutual recognition principles established under the CIPM MRA, laboratory performance is fundamentally assessed through the ability to demonstrate compatibility of results via En ratios. Accordingly, it is important to assess how the optimized conditions contribute to enhanced measurement comparability and improved conformity with international metrological expectations. The optimized environmental and operational settings identified in this study have direct implications for interlaboratory comparability, particularly through their influence on En ratios. By minimizing operator presence, stabilizing temperature, and controlling illuminance, the optimized conditions reduce variability in air density, buoyancy corrections, and convection effects, thereby lowering both Type A and environmental uncertainty components. A reduction in these contributors directly decreases the combined standard uncertainty used in En ratio calculations, increasing the likelihood of achieving $|E_n| < 1$. Although no formal comparison is undertaken here, the optimized settings move the laboratory closer to its minimum achievable uncertainty, providing a strong basis for improved metrological equivalence and alignment with OIML and CIPM MRA requirements.

IV. CONCLUSION

This study successfully optimized laboratory environmental parameters to improve the quality of 1 kg artifact and gravimetric testing using the Taguchi method and Response Surface Methodology (RSM). The optimization results indicate that the best combination for laboratory conditions includes an AC temperature of 16°C, an actualization duration of 15 minutes, a lighting intensity of 50%, and one operator in the laboratory. ANOVA analysis confirmed that AC temperature is the most influential factor on the response variables, followed by lighting and the number of people, while time has a lesser impact. The obtained regression model demonstrates a linear relationship between the independent variables and responses, with AC temperature being the dominant factor in increasing both artifact and gravimetric values.

The contour and surface plots further support these findings, showing that an increase in AC temperature and lighting contributes to higher artifact and gravimetric values. Additionally, the desirability analysis resulted in a D value of 0.869, indicating a high degree of alignment between the selected optimization conditions and the desired targets. Therefore, this study provides an Internet of Things (IoT)-based solution for effectively controlling laboratory environmental conditions, reducing variability in test results, and enhancing the quality and consistency of legal metrology artifacts.

The results indicate that the optimization model developed for both the mass artifact and gravimetric responses is robust and metrologically traceable within the

evaluated measurement-uncertainty limits. The combined expanded uncertainty, derived in accordance with [34], [35], [36], does not alter the optimum condition identified through the Taguchi-RSM analysis. Instead, it confirms that the observed variability in desirability lies within the expected range of measurement uncertainty. Therefore, the final optimum can be considered statistically valid, metrologically traceable, and practically reproducible under controlled laboratory conditions.

Overall, the Taguchi-RSM framework presented in this study provides a complementary optimization capability that extends beyond conventional environmental control guidelines, enabling calibration laboratories to actively refine environmental and operational conditions to reduce measurement variability, strengthen metrological robustness, and enhance practical laboratory performance.

REFERENCES

[1] M. Cakmakci, N. M. Durakbasa, M. Kemal Karasu, and G. Bas, "The relationship between the quality engineering and Taguchi methodology," in *11th International Symposium on Measurement and Quality Control*, 2013, pp. 1–4.

[2] Arif Nurjaya, "Analisis Control Chart Dalam Program Jaminan Kesesuaian Hasil Pengukuran," *Insan Metrologi PPSDK*, vol. 1, no. 1, pp. 20–27, Dec. 2021, doi: 10.55101/ppsdk.v1i1.575.

[3] R. Manohara, M. A. Harinath, and P. G. Scholar, "Application of Taguchi Method for Optimization of Process Parameters in Drilling Operation," *International Journal of Trend in Scientific Research and Development*, vol. 3, no. 4, pp. 1052–1057, 2019, [Online]. Available: http://creativecommons.org/licenses/by/4.0

[4] O. F. Aje and A. J. Adie, "Response surface methodology and Taguchi method based applications – A Review," *Global Journal of Engineering and Technology Advances*, vol. 2020, no. 01, pp. 53–059, 2020, doi: 10.30574/gjeta.

[5] M. Aravind and S. Periyasamy, "Optimization of Surface Grinding Process Parameters By Taguchi Method And Response Surface Methodology," *International Journal of Engineering Research and Technology*, vol. 3, no. 5, pp. 1721–1727, 2014, [Online]. Available: www.ijert.org

[6] A. T. Lase and H. Pranoto, "A Review on CNC Milling Parameter Optimization Using Taguchi and Response Surface Methodology (RSM)," *International Journal of Advanced Technology in Mechanical, Mechatronics and Materials (IJATEC)*, vol. 06, no. 1, pp. 34–41, 2025, doi: 10.37869/ijatec.v6i1.108.

[7] S. V Alagarsamy and N. Rajakumar, "Analysis of Influence of Turning Process Parameters on MRR & Surface Roughness Of AA7075 Using Taguchi's Method and Rsm," 2014. [Online]. Available: www.ijars.in

[8] Y. T. Jou, W. T. Lin, W. C. Lee, and T. M. Yeh, "Integrating the taguchi method and response surface methodology for process parameter optimization of the injection molding," *Applied Mathematics and Information Sciences*, vol. 8, no. 3, pp. 1277–1285, May 2014, doi: 10.12785/amis/080342.

[9] P. Kumari, D. Majhi, B. Ranjan Rout, and S. Ahmed, "Analysis of resistance spot welding using multi-objective Taguchi method and RSM," 2019. [Online]. Available: www.ijres.org

[10] J. S. Makwana, "Comparative Analysis for Power Consumption Optimization of CNC Turned Part Using Response Surface Methodology and Taguchi's Technique," *International Journal of Research and Analytical Reviews*, 2022, [Online]. Available: www.ijrar.org

[11] M. S. M. Said, S. M. Kassim, Si. H. Tomadi, and C. H. C. Haron, "Comparison between Taguchi Method and Response Surface Methodology In Optimizing Machining Condition," *International Conference on Robust Quality Engineering*, pp. 60–64, 2013.

[12] M. Santhanakumar and R. Adalarasan, "Application of grey taguchi based response surface methodology (GT-RSM) in injection moulding of polypropylene/E-glass composite," *International Journal of Manufacturing, Materials, and Mechanical Engineering*, vol. 5, no. 1, pp. 35–48, Jan. 2015, doi: 10.4018/ijmmme.2015010103.

[13] G. R. Mugagga, I. B. Omosa, and T. Thoruwa, "Optimization and Analysis of a Low-Pressure Water Scrubbing Biogas Upgrading System via the Taguchi and Response Surface Methodology Approaches," *International Journal of Renewable Energy Development*, vol. 12, no. 1, pp. 99–110, Jan. 2023, doi: 10.14710/ijred.2023.48269.

[14] R. Viswanathan and S. Ramesh, "Optimization of Machining Parameters for Magnesium Alloy using Taguchi Approach and RSM," 2014, doi: 10.13140/2.1.1515.6801.

[15] L. L. R Rodrigues and M. Brn, "Optimization of the Process Parameters to Minimize the Surface Roughness in Drilling of CFRP Composites using Taguchi Method and RSM," 2013. [Online]. Available: http://inpressco.com/category/ijcet

[16] B. Özturk, Ş. Kaymak, and Ö. Kucuk, "The Taguchi and RSM Based Optimization of Energy Consumption On Internal Gear Pumps," *International Journal of 3D Printing Technologies and Digital Industry*, vol. 6, no. 1, pp. 164–175, Apr. 2022, doi: 10.46519/ij3dptdi.1001245.

[17] H. Mugutkar and N. Tamiloli, "Application of taguchi and RSM parameters on surface roughness and material removal rate of AA6082T6," in *Journal of Physics: Conference Series*, IOP Publishing Ltd, Nov. 2021. doi: 10.1088/1742-6596/2070/1/012211.

[18] Y. Fedai, "Optimization of Drilling Parameters in Drilling of MWCNT-Reinforced GFRP Nanocomposites Using Fuzzy AHP-Weighted Taguchi-Based MCDM Methods," *Processes*, vol. 11, no. 10, Oct. 2023, doi: 10.3390/pr11102872.

[19] J. Laxman and K. G. Raj, "Mathematical modeling and analysis of EDM process parameters based on Taguchi design of experiments," in *Journal of Physics: Conference Series*, Institute of Physics Publishing, Dec. 2015. doi: 10.1088/1742-6596/662/1/012025.

[20] A. Kolakoti, M. Setiyo, and M. L. Rochman, "A Green Heterogeneous Catalyst Production and Characterization for Biodiesel Production using RSM and ANN Approach," *International Journal of Renewable Energy Development*, vol. 11, no. 3, pp. 703–712, Aug. 2022, doi: 10.14710/ijred.2022.43627.

[21] P. Rajamani, K. Sunitha, D. V Srikanth, and M. S. Rao, "Approach of Taguchi, RSM &ANOVA Using Stat Graphics on Machining of Ceramics with Abrasive Jet Drilling," *International Journal of Scientific Research in Multidisciplinary Studies*, vol. 6, no. 1, pp. 46–49, 2020, [Online]. Available: www.isroset.org

[22] S. Arhamnamazi, F. Aymerich, P. Buonadonna, M. El Mehtedi, and H. Taheri, "Application of Central Composite Design in the Drilling Process of Carbon Fiber-Reinforced Polymer Composite," *Applied Sciences (Switzerland)*, vol. 14, no. 17, Sep. 2024, doi: 10.3390/app14177610.

[23] S. Kumar and B. B. Vashist, "Understanding the concept of Taguchi Technique Optimization of Material Surface Roughness and Removal Rate for metals in CNC Turning Operation: A Review," *RESEARCH REVIEW International Journal of Multidisciplinary*, vol. 7, no. 1, pp. 49–52, Jan. 2022, doi: 10.31305/rrijm.2022.v07.i01.006.

[24] V. Nguyen, D. Nguyen, D. Do, and T. Tran, "Multi-Objective Optimization of the Surface Grinding Process for Heat-Treated Steel," *International Journal of Automotive and Mechanical Engineering*, vol. 21, no. 4, pp. 11831–11843, 2024, doi: 10.15282/IJAME.21.4.2024.8.0911.

[25] R. Wang, X. Xiong, H. Liang, and J. Zhang, "Optimization Design of Redundant Parallel Posture Adjustment Mechanism for Solar Wing Docking Based on Response Surface Methodology," *Applied Sciences (Switzerland)*, vol. 14, no. 17, Sep. 2024, doi: 10.3390/app14178059.

[26] F. Härtig, K. Lehrmann, and R. Tutsch, "Simulated measurement-uncertainty determination for mass-standard calibration via transfer artefacts," in *Measurement: Sensors*, Elsevier Ltd, Dec. 2021. doi: 10.1016/j.measen.2021.100090.

[27] K. Lehrmann, F. Härtig, and R. Tutsch, "Numerical simulation for determining the measurement uncertainty for the calibration of mass standards by transfer artefacts," *Measurement: Sensors*, vol. 24, Dec. 2022, doi: 10.1016/j.measen.2022.100414.

[28] R. Green, S. Davidson, J. Liard, N. Murnaghan, D. A. Castro, and H. Parks, "Realisation and dissemination of mass through the consensus value of the kilogram and preparation for the final phase of traceability to independent realisations," in *Measurement: Sensors*, Elsevier Ltd, 2024. doi: 10.1016/j.measen.2024.101352.

[29] E. Batista, V. Silverio, K. Romieu, J. Alves e Sousa, and T. S. Daugbjerg, "Development of measurement procedures for volume and flow related quantities in microfluidic devices," in *Measurement: Sensors*, Elsevier Ltd, 2024. doi: 10.1016/j.measen.2024.101551.

[30] A. Archenti, W. Gao, A. Donmez, E. Savio, and N. Irino, "Integrated metrology for advanced manufacturing," *CIRP Annals*, vol. 73, no. 2, pp. 639–665, Jan. 2024, doi: 10.1016/j.cirp.2024.05.003.
[31] R. Rai, R. R. Sahoo, D. Kumar, and H. S. Bhatia, "Diesel Engine Performance and Emission Parameters Optimization Using Taguchi and Response Surface Methodology," in *Transactions of the Royal Institution of Naval Architects Part A: International Journal of Maritime Engineering*, University of Buckingham Press, 2024, pp. A305–A314. doi: 10.5750/ijme.v1i1.1362.
[32] D. Métrologie Légale, "Metrological and technical requirements," in *OIML 111-1 Edition 2004*, 2004. [Online]. Available: www.oiml.org
[33] D. Métrologie Légale, "Standard capacity measures for testing measuring systems for liquids other than water (OIML)," in *OIML R 120 Edition 2010 (E)*, 2010.
[34] International Organization of Legal Metrology, "OIML R-111:2004 (E) — Weights of Classes E1, E2, F1, F2, M1, M2, M3," Paris, France, 2004.
[35] International Organization of Legal Metrology, "OIML R-120:2020 (E) — Standard for Weighing Instruments," Paris, France, 2020.
[36] Joint Committee for Guides in Metrology, "JCGM 100:2008 — Evaluation of Measurement Data — Guide to the Expression of Uncertainty in Measurement (GUM)," Sèvres, France, 2008.



Saufik Luthfianto earned his doctoral degree in Industrial Engineering from Universitas Sebelas Maret (UNS), Surakarta, Indonesia. He is currently affiliated with the Industrial Engineering Study Program, Universitas Pancasakti Tegal, Tegal, Indonesia. His research interests span quality engineering, manufacturing process experimentation, sustainable manufacturing optimization through statistical data analysis, and biomaterials research utilizing the Taguchi method and multi-objective optimization. (email: saufik_lutfianto@upstegal.ac.id).



Sandi Satria received his Bachelor's degree in Industrial Engineering from Universitas Pancasakti Tegal (expected graduation in 2025). Since 2013, he has been working in the Government's Legal Metrology Office, officially authorized by the Minister of Trade as a Verification Officer (initials mark "ot") in the field of mass and volume transactions in Tegal City, Central Java, Indonesia. His recent research focuses on implementing the Internet of Things (IoT) to regulate optimal temperature and humidity in mass laboratories. (email: beginsucces@gmail.com).



Irfan Santoso completed his Ph.D. in Mechanical Engineering at Universitas Sebelas Maret (UNS), Surakarta, Indonesia. He is currently affiliated with the Mechanical Engineering Study Program, Universitas Pancasakti Tegal, Tegal, Central Java, Indonesia. His research interests cover mechanical design, manufacturing processes, materials engineering, and experimental investigations in engineering applications. (email: irfansantosa@upstegal.ac.id).